

Non-Markovian Quantum Dynamics and Classical Chaos

Ignacio García-Mata,^{1,2} Carlos Pineda,³ and Diego Wisniacki⁴

¹*Instituto de Investigaciones Físicas de Mar del Plata (IFIMAR, CONICET),
Universidad Nacional de Mar del Plata, Mar del Plata, Argentina.**

²*Consejo Nacional de Investigaciones Científicas y Tecnológicas (CONICET), Argentina*

³*Instituto de Física, Universidad Nacional Autónoma de México, México D.F., 01000, México*

⁴*Departamento de Física “J. J. Giambiagi”, FCEN, Universidad de Buenos Aires, 1428 Buenos Aires, Argentina*

(Dated: August 3, 2018)

We study the influence of a chaotic environment in the evolution of an open quantum system. We show that there is an inverse relation between chaos and non-Markovianity. In particular, we remark on the deep relation of the short time non-Markovian behavior with the revivals of the average fidelity amplitude – a fundamental quantity used to measure sensitivity to perturbations, and to identify quantum chaos. The long time behavior is established as a finite size effect which vanishes for large enough environments.

PACS numbers: 03.65.Yz, 05.45.Mt, 05.45.Pq

I. INTRODUCTION

The advent of quantum information and quantum technology has brought us to a deeper understanding of the basics of quantum mechanics. As a result, various fundamental aspects, such as equilibration [1], simulability [2], and even foundations [3], have been revised. This framework has provided both valuable insight into the foundations and new technological achievements. But theory and its related experiments have advanced asymmetrically mainly due to the impossibility to isolate completely the experimental setup, leaving the system ‘open’ and exposed to decoherence [4].

Many quantum open systems problems can be solved after assumptions are made. The widely used Born-Markov approximation, successfully applied to describe many physical situations [5], is associated with both a memory-less environment and a weak coupling between system and environment. However, recently, interest in quantum open systems where this assumption no longer applies – usually called non-Markovian (NM) evolution – has flourished [6–8].

A natural question to ask is to what extent the dynamical properties of the environment can extend the validity of the Born-Markov approximation, even beyond the weak coupling regime. In other words, how well does a chaotic environment reproduce Markovian evolution. In this paper, we address this question analytically and numerically by means of a probe qubit coupled to a generic environment where different degrees of chaos can be tested. Exploring the time evolution of non-Markovianity measures, we show that the stronger the chaos in the environment, the more Markovian the evolution is. We build upon previous knowledge [9, 10] of measurable quantities such as the fidelity amplitude which can be directly related to recently proposed measures of NM behavior. Moreover, we establish that the short time behavior of the fidelity amplitude determines the characteristics of the qualitative NM behavior. The lingering, long time contributions, are finite size effects which contribute only as a linear term with a slope

that goes to zero as the environment size goes to infinity. The remaining non-Markovianity is thus size independent and due to short time revivals in the fidelity amplitude decay.

The paper is organized as follows. In Sect. II we describe the system we use for our analysis. It consists of a qubit in the presence of an environment whose evolution is subject to the state of the qubit. In Sect. III we briefly describe the Non-Markovianity measure based on distinguishability and its relation to the fidelity decay of the environment. The numerical results and analysis are done in Sect. IV and we present some concluding remarks in Sect. V.

II. SYSTEM

We consider a system-environment situation, whose Hilbert space is $\mathcal{H} = \mathcal{H}_{\text{sys}} \otimes \mathcal{H}_{\text{env}}$, where \mathcal{H}_{sys} and \mathcal{H}_{env} denote system and environment. Any Hamiltonian can then be split as

$$H = H_{\text{sys}} + H_{\text{env}} + \varepsilon V_{\text{sys,env}}, \quad (1)$$

where ε is real and controls the strength of the interaction between system and environment. We further restrict to the case in which \mathcal{H}_{sys} represents a qubit, i.e. when $\dim \mathcal{H}_{\text{sys}} = 2$, and we call $N = \dim \mathcal{H}_{\text{env}}$. The choice of the terms in Eq. (1) results in different physical situations. However, instead of specifying the particular form of Eq. (1), we shall impose two general conditions. The first one involves the nature of the interaction. We shall assume that it is factorizable, i.e. that $V_{\text{sys,env}} = V_{\text{sys}} \otimes V_{\text{env}}$. Such structure appears in a wide variety of situations, including Ising interaction and atom-field interaction under various approximations [11]. The second assumption is to consider that the evolution of the central system, \mathcal{H}_{sys} , either occurs at much smaller time scales than that in which decoherence occurs or that it is a multiple of V_{sys} . In the former, one can safely ignore the contribution to the dynamics, and in the latter case, H_{sys} can be included in the interaction term and can keep the factorizable structure unaffected. This occurs, e.g. in the case of a strong magnetic field applied to a set of interacting spins and thus is of particular importance in, among others, nuclear magnetic resonance

* i.garcia-mata@conicet.gov.ar

(NMR). In this situation, one can write

$$H = |0\rangle\langle 0| \otimes H_0 + |1\rangle\langle 1| \otimes H_1 \quad (2)$$

with H_0 and H_1 acting only on the environment and both $|0\rangle\langle 0|$, $|1\rangle\langle 1|$ being projectors onto some orthonormal basis of the qubit. This Hamiltonian has already been introduced in [12] and can be interpreted as having an environment whose evolution is conditioned by the state of the qubit. The initial state of the system shall be $\rho_{\text{sys,env}}(0) = \rho_{\text{sys}}(0) \otimes \rho_{\text{env}}$. Notice that the only condition imposed on the initial state is that it be a product state. The evolution of the qubit is

$$\rho_{\text{sys}}(t) = \text{Tr}_{\text{env}} [U(t)\rho_{\text{sys}}(0) \otimes \rho_{\text{env}}U^\dagger(t)] \quad (3)$$

with

$$U(t) = |0\rangle\langle 0|U_0(t) + |1\rangle\langle 1|U_1(t) \quad (4)$$

and $U_j(t) = \exp(-itH_j/\hbar)$. It is convenient to rephrase Eq. (3) in terms of a quantum channel

$$\rho_{\text{sys}}(t) = \Lambda(t)[\rho_{\text{sys}}(0)] \quad (5)$$

Notice that although $\Lambda(t)$ results from tracing out the environment it still depends on ρ_{env} .

The matrix elements of the channel induced by Eq. (3), in the Pauli basis are

$$\Lambda_{j,k}^{(t)} = \frac{1}{2} \text{Tr} [\sigma_j U(t) \sigma_k \otimes \rho_{\text{env}} U^\dagger(t)]. \quad (6)$$

If we take $\sigma_0 = \mathbb{I}$ and $\sigma_{1,2,3} = \sigma_{x,y,z}$, the channel takes the simple form

$$\Lambda = \begin{pmatrix} 1 & 0 & 0 & 0 \\ 0 & \Re[f(t)] & \Im[f(t)] & 0 \\ 0 & \Im[f(t)] & \Re[f(t)] & 0 \\ 0 & 0 & 0 & 1 \end{pmatrix}. \quad (7)$$

with $f(t) = \text{Tr}[\rho_{\text{env}}U_1(t)^\dagger U_0(t)]$ being the expectation value of the echo operator. If ρ_{env} is a pure state [10] then $|f(t)|^2$ is the Loschmidt echo (LE) [13] – also called fidelity – originally proposed to measure sensitivity to perturbations in the Hamiltonian as a signature of quantum chaos [14]. The LE decays as a function of time and the – more or less – universal decay regimes have been extensively studied (see reviews [15, 16]). The environment could in fact be in a pure state – e.g. in a thermal ground state at zero temperature. However it is probably easier to imagine the environment being in a mixed state – e.g. at thermal equilibrium at a given temperature. We choose then the environment to be in the maximally mixed state, i.e. proportional to the identity. In that case we obtain the real and imaginary part of the average fidelity amplitude (AFA),

$$\langle f(t) \rangle = \frac{1}{N} \text{Tr}[U_1(t)^\dagger U_0(t)] \quad (8)$$

i.e. the average value of the echo operator with respect to an orthonormal basis. We remark that the choice of basis (or any complete set) is arbitrary. This fact contrasts the case of the LE where the *kind* of states in the set is crucial [21].

III. FIDELITY AMPLITUDE MEASURES NON-MARKOVIAN BEHAVIOR

During a classical Markovian process the distance between two initial distributions decreases monotonically. Deviations from this behavior are a landmark of non-Markovianity. Breuer *et al.* [7] used this property to *define* a measure of NM behavior in a quantum setting. The distance can be chosen as to link non-Markovianity with distinguishability of states and thus information flow between the system and its surroundings. Such a measure is defined as

$$\mathcal{M} = \max_{\rho_{1,2}(0)} \int_{\sigma>0} dt \sigma(t, \rho_{1,2}(0)), \quad (9)$$

where $\sigma(t, \rho_{1,2}(0)) = dD(\rho_1(t), \rho_2(t))/dt$ is the rate of change of the trace distance

$$D(\rho_1(t), \rho_2(t)) = \frac{1}{2} \text{tr} |\rho_1(t) - \rho_2(t)| \quad (10)$$

between initial states $\rho_{1,2}(0)$. In [8] two other measures were proposed, based on deviation of semi-group properties of quantum flows. Both study the physicality of the induced instant map at intermediate times, one via the Jamiołkowski isomorphism and the other via the entanglement (as measured with the concurrence) with an ancilla qubit. It is straightforward to show that for channels like Eq. (7) the measure induced by the entanglement is proportional to \mathcal{M} .

In our case, the states that maximize \mathcal{M} are $\rho_{\pm} = (I \pm (a\sigma_x + b\sigma_y))/2$, with $|a|^2 + |b|^2 = 1$, leading to

$$\mathcal{M} = 2 \int_{|f|>0} \frac{d|\langle f(t) \rangle|}{dt}. \quad (11)$$

In other words, Eq. (11) means that NM behavior is directly related to the positive derivative of the AFA as a function of time [17].

For fully chaotic systems both the AFA and the LE saturate around a value that depends on \hbar . After saturation sets in, the state is approximately random and the value of both fidelity and fidelity amplitude fluctuate. As a consequence, we expect the NM measure to grow indefinitely. Thus in our calculations of \mathcal{M} we modify the original definition in [7] and calculate the NM measure up to a certain time. Regardless, the measure at time t still holds its meaning, i.e. the larger $\mathcal{M}(t)$ means the distance between the two states has ceased to decrease (or increased) more in that period of time, which implies a more NM behavior.

IV. NON-MARKOVIANITY AND CHAOS: RESULTS

Now we consider the long standing question of the relation between chaos and Markovianity. To do so we model the environment using simple but fully featured systems: quantum maps on the torus. The quantization of the torus implies that both position and momentum are discretized and the effective Planck constant is the inverse of the Hilbert space dimension

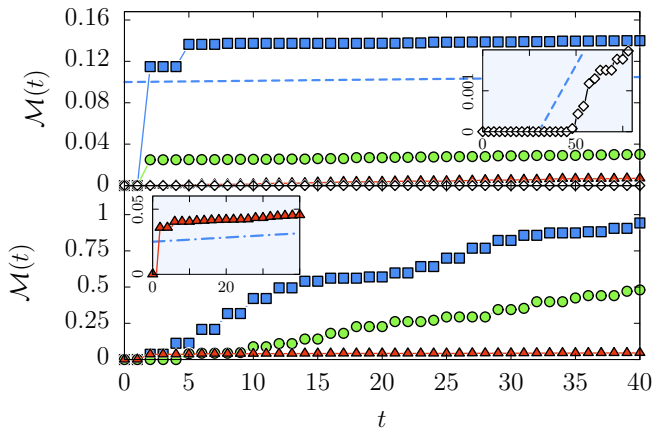


FIG. 1. (color online) $\mathcal{M}(t)$ for the PCM (top) and the HM (bottom). Top: (squares) $\lambda = 0.96$, (circles) $\lambda = 1.76$, (triangles) $\lambda = 5.99$. $\delta K/\hbar = 3.635$. (diamonds) $\lambda = 0.96$, $\delta K/\hbar = 0.64$ (weak coupling). Bottom: (squares) $k = 0.001$ (regular), (circles) $k = 0.25$ (mixed), (triangle) $k = 1$ (fully chaotic). Top inset: (diamonds) weak coupling case. Bottom inset: (triangles) $k = 1$, note the linear dependence. The slopes of the straight lines are $\alpha = 1/2N$ (top panel, dashed) and $\alpha = 2/3N$ (bottom inset, dot-dash). $N = 4096$.

N . In this setting, a quantum map is simply a unitary U acting on an N dimensional Hilbert space.

We consider two different maps. First, the quantum perturbed cat map (PCM)

$$U_{c,K} = e^{-i\pi N a \hat{p}^2} e^{i\pi N a \hat{q}^2} e^{i\pi N K (2 \sin(2\pi \hat{q}) - \sin(4\pi \hat{q}))} \quad (12)$$

where \hat{q} and \hat{p} are the generators of periodic position and momentum translations on the torus with discrete eigenvalues $0, 1/N, \dots, (N-1)/N$. The subindex K denotes the depth of the kicking potential. For $a = 1$ and $K = 0$ it is the quantum version of Arnold's cat map, a uniformly hyperbolic and mixing map of the torus onto itself, which is a paradigmatic example of chaos in two dimensions. The positive Lyapunov exponent λ , which determines the rate of exponential divergence of classical trajectories, is uniform over the whole phase space. We explore different degrees of chaos by changing a since, for small K , $\lambda \approx \ln((2 + a^2 + \sqrt{a^2(4 + a^2)})/2)$. Here $U(t) \equiv U^t$ where now t is an integer, and $U_0 = U_{c,K}$ and $U_1 = U_{c,K+\delta K}$.

The other map we consider is

$$U_{H,k,k'} = e^{iNk \cos(2\pi \hat{q})} e^{iNk' \cos(2\pi \hat{p})} \quad (13)$$

which corresponds to the Harper map (HM) [18]. It is an approximation of the motion of an electron in a crystal under the action of an external field [19]. For $k \lesssim 0.11$, the dynamics described by the associated classical map is regular, while for $k \gtrsim 0.63$ there are no remaining visible regular islands. We set $U_0 = U_{H,k,k}$ and $U_1 = U_{H,k+\delta k,k}$.

We now take the result of Eq. (11) and compute numerically $\mathcal{M}(t)$ for the two maps. Notice that the structure of the maps is $U_1 = U_0 P(\varepsilon)$ (with $\varepsilon = \delta K$ or δk). The $\varepsilon \rightarrow 0$ limit implies $P(\varepsilon)[\text{and } f(t)] \rightarrow 1$ (i.e. no decoherence). The coupling strength is given by δK and δk . For weak couplings, (in the chaotic case) the AFA decays exponentially, and the

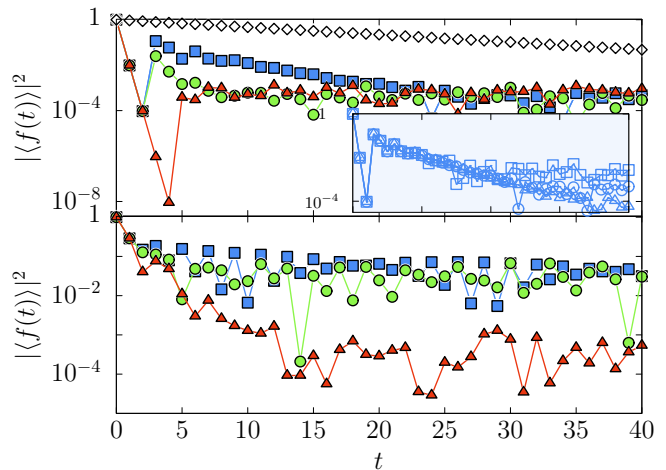


FIG. 2. (Color online) $|\langle f(t) \rangle|^2$, same cases as Fig. 1 for the PCM (top) and the HM (bottom). Inset: $\lambda = 0.96$ for the PCM, for $N = 512, 4096, 16384$.

rate depends quadratically on the coupling parameter – the Fermi golden rule regime (FGR). Here the evolution is expected to be Markovian. Throughout this paper we consider mainly coupling strengths beyond the FGR.

The AFA is evaluated directly by averaging the echo operator over a complete set of states. For the PCM we change a in Eq. (12) so we can assess the change in \mathcal{M} for different levels of chaoticity. For the HM varying k in Eq. (13), we go from integrable to completely chaotic. In Fig. 1 (top), we show the NM measure $\mathcal{M}(t)$ for three different examples of the PCM with varying degrees of chaoticity. On the bottom of Fig. 1, we show the same for the HM, where we show the AFA for three different k (regular, mixed, and chaotic). For the PCM after a small number of steps, there appear three distinct jumps. As expected, the larger λ is, the smaller is the jump, which confirms the intuitive relation that the more chaotic the environment is, the more Markovian is the evolution. After this short time behavior, the three cases exhibit linear growth of $\mathcal{M}(t)$. The explanation is simple. For fully chaotic systems, at a time of the order of Ehrenfest time [$t_E = \ln(1/\hbar)/\lambda$], the AFA saturates – but oscillates – around $1/N$. This saturation corresponds to the overlap between two completely random states, and is approximately constant. This implies that \mathcal{M} will grow linearly and that the slope α will be proportional to $1/N$. The proportionality constant depends on the map (for the PCM, regardless of the value of λ , we found the slope to be $\alpha \approx 1/2N$). For completeness, we include the case $\lambda = 0.96$ in the weak coupling regime. As expected, $\mathcal{M}(t) = 0$ visibly up to $t \approx 50$. After that we have linear growth. On the bottom of Fig. 1, we show $\mathcal{M}(t)$ for the HM for three qualitatively different cases. In the case in which the classical dynamics is regular ($k = 0.001$), we observe that up to the times shown $\mathcal{M}(t)$ increases non-linearly. There is a saturation of the AFA, but *not* at $1/N$, which eventually leads to a linear growth of \mathcal{M} . This saturation for small k takes place at much larger times. When the dynamics is almost fully chaotic ($k = 1$), there is a very small jump after

which there remains only the linear growth due to fluctuations around the saturation value. The slope of this linear growth is $\alpha \approx 2/3N$. In the parameter region where the KAM tori of the HM begin to break, there is a combination between regular and chaotic dynamics (initial states can have components inside regular islands and components inside the chaotic sea) and the behavior is less intuitive. In fact what is observed – in Fig. 1 for $k = 0.25$ – is that the environment modeled by a HM in the transition from regular to chaotic can be strongly non-Markovian [see also Fig. 3].

In both situations, the long time behavior for the NM measure is linear. This would imply $\mathcal{M} \rightarrow \infty$. However, this assertion presents no problems in our analysis. The slope of the long time linear regime goes to zero as N grows. Intuition suggests ‘large’ environment as a necessary condition of Markovianity. However, in the $N \rightarrow \infty$ limit, there will always remain the short time value attained by \mathcal{M} (see Fig. 1), which is independent of N (Fig. 2).

To shed more light on the results displayed in Fig. 1 we focus on the evolution of the AFA as a function of time for the cases considered above. In Fig. 2 we show examples of the decay of the square of the AFA. In the top panel, we show results for the PCM for three different values of λ (i.e. different a in Eq. (12)). In the bottom panel, we show the same for the HM, with three values of k (regular, mixed, and chaotic). In contrast with the LE, the AFA is independent of the type if initial states and decays exponentially with two distinct decay rates. The short time decay rate Γ can be related to uncorrelated – random – dynamics [9]. The value of Γ can be computed using semiclassical methods. This decay rate can diverge, meaning that the short time decay can be extremely fast. These divergences – which depend on the type of perturbation, and are more evident the larger λ is – could be related to the phenomenon known as survival collapse [20] after which the largest revivals appear. For the numerical results, on the top we chose a value of δk for the PCM which corresponds to a large Γ (near the diverging values), where the largest revivals have been observed [9, 21]. We remark, moreover, that the short time decay of the AFA is independent of N and therefore so is the revival. In the inset of Fig. 2 we see that the AFA (for the PCM, with $\lambda = 0.96$) is almost equal for three different values of N up to $t \approx 10$. This is important because the short time revivals will provide the main contribution to \mathcal{M} . While this contribution remains constant with N the long time contribution goes to zero as $1/N$. The curve with diamonds supports the results shown in Fig. 1 [top] for the weak coupling regime.

The possibility to assess the behavior as an environment model, by changing one parameter, from regular to chaotic, is indeed tempting. In Fig. 3 we computed \mathcal{M} at a fixed time for the HM for different values of k . We chose $t = 20$, around the time in which the fastest decaying case starts to saturate (see Fig 2, bottom). We see that for small k (regular dynamics), \mathcal{M} takes a constant value (which, apart from the fixed time, depends on N and δK) and there is a transition where \mathcal{M} depends on k just where the KAM tori begin to break. When the dynamics is fully chaotic, the value of \mathcal{M} (at $t = 20$) again takes a constant value. Fig. 3 is a clear example of the

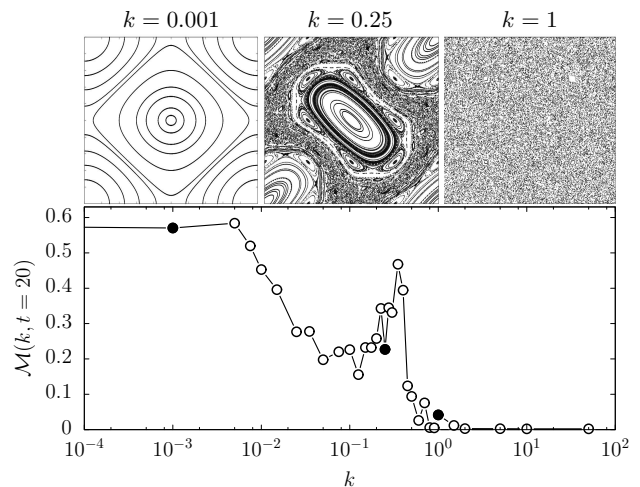


FIG. 3. $\mathcal{M}(t = 20)$ as a function of k , for $t = 20$, for the HM with $N = 4096$ and $\delta k = 0.00113$. Top: phase space diagram for three examples of k : regular, $k = 0.001$; mixed $k = 0.25$; chaotic $k = 1$. The corresponding points in the bottom panel are drawn in solid black.

expected behavior: regular environments are expected to be more NM while the NM behavior that appears to linger in the chaotic regime is due to the same oscillatory behavior around the saturation value mentioned for the case of the PCM. In the transition region, $0.11 \lesssim k \lesssim 0.63$, there is coexistence between tori and chaotic regions. In the first place, the existence of regular islands implies that even though there will be leaking – by tunneling – to the chaotic regions, the saturation will take much longer. In addition, the area occupied by the chaotic region is smaller than the torus, therefore, the saturation value is larger than $1/N$. We have checked for other times (up to $t \sim 1000$) and also other methods (not shown) – e.g. taking as NM value the y-intercept of an asymptotic linear fit – and the qualitative behavior is the same. Further studies are needed in order to fully grasp the behavior in the intermediate region.

V. CONCLUSIONS

We addressed the issue of how well a chaotic environment can model Markovian evolution. We used a probe qubit as a system coupled to an environment modeled by a quantum map. In this setting there is a straightforward relation between some measures of NM behavior and the AFA. The study of the time evolution of the NM measure has shown that the stronger the chaos of the environment (in the PCM larger λ), the more Markovian the evolution will be, even if the coupling is strong. Furthermore, there are two well defined regimes. For short times, there is no dependence with N and the NM is measured by revivals in the AFA. In contrast, for large times, the measure grows linearly with a slope that vanishes as $\propto 1/N$. Thus, in accordance with [22], as $N \rightarrow \infty$ there can be a remaining non vanishing value for non-Markovianity, for a chaotic environment. The revivals of the LE were recently related to NM behavior [10]. Here we make a more general approach

by allowing the bath to be in a thermal state and expressing non-Markovianity in terms of the AFA – a quantity which is independent of the set of states over which the average is done.

UNAM-PAPIIT IN117310. I.G.M. and D.A.W. received support from ANCyPT (PICT 2010-1556), UBACyT, and CONICET (PIP 114-20110100048 and PIP 11220080100728).

ACKNOWLEDGMENTS

Discussions with P. Haikka and J. Piilo are acknowledged. C.P. received support from the projects CONACyT 57334 and

-
- [1] A. Riera *et al.*, Phys. Rev. Lett. **108**, 080402 (2012).
 [2] J. I. Latorre, J. Phys. A: Math. Theo. **40**, 6689 (2007).
 [3] G. Chiribella *et al.*, Phys. Rev. A **84**, 012311 (2011).
 [4] W. H. Zurek, Rev. Mod. Phys. **75**, 715 (2003).
 [5] H. Breuer and F. Petruccione, *The Theory of Open Quantum Systems* (Oxford University Press, Oxford, 2007).
 [6] S. Daffer *et al.*, Phys. Rev. A **70**, 010304 (2004).
 [7] H.-P. Breuer *et al.*, Phys. Rev. Lett. **103**, 210401 (2009).
 [8] A. Rivas *et al.*, Phys. Rev. Lett. **105**, 050403 (2010).
 [9] I. García-Mata *et al.*, New J. Phys. **13**, 103040 (2011).
 [10] P. Haikka *et al.*, Phys. Rev. A **85**, 060101(R) (2012).
 [11] M. O. Scully and M. S. Zubairy, *Quantum Optics*, 1st ed. (Cambridge University Press, 1997).
 [12] Z. P. Karkuszewski *et al.*, Phys. Rev. Lett. **89**, 170405 (2002).
 [13] R. A. Jalabert and H. M. Pastawski, Phys. Rev. Lett. **86**, 2490 (2001).
 [14] A. Peres, Phys. Rev. A **30**, 1610 (1984).
 [15] T. Gorin *et al.*, Phys. Rep. **435**, 33 (2006).
 [16] Ph. Jacquod and C. Petitjean, Adv. Phys. **58**, 67 (2009).
 [17] While in the process of writing this manuscript, this relation was independently established in [10].
 [18] P. Leboeuf *et al.*, Phys. Rev. Lett. **65**, 3076 (1990).
 [19] R. Artuso, Scholarpedia **6**, 10462 (2011).
 [20] E. R. Fiori and H. Pastawski, Chem. Phys. Lett. **420**, 35 (2006).
 [21] I. García-Mata and D. A. Wisniacki, J. Phys. A: Math. Theor. **44**, 315101 (2011).
 [22] M. Žnidarič *et al.*, Phys. Rev. Lett. **107**, 080404 (2011).